

# Effect of adhesive composition on bonding of silicon nitride ceramic

Fei Zhou\*

*School of Materials Science and Engineering, Jiangsu University, Zhenjiang 212013, PR China*

Received 2 August 2001; received in revised form 2 May 2002; accepted 12 June 2002

## Abstract

$\text{Si}_3\text{N}_4$ – $\text{Si}_3\text{N}_4$  ceramics were bonded by using  $\text{Y}_2\text{O}_3$ – $\text{Al}_2\text{O}_3$ – $\text{SiO}_2$ ,  $\text{Y}_2\text{O}_3$ – $\text{La}_2\text{O}_3$ – $\text{Al}_2\text{O}_3$ – $\text{SiO}_2$ ,  $\text{Y}_2\text{O}_3$ – $\text{CeO}_2$ – $\text{Al}_2\text{O}_3$ – $\text{SiO}_2$  solders. Joining was carried out at 1823 K for 15 min at atmospheric pressure. The effects of adhesive composition on interfacial wetting and joint strength were investigated. The microstructure and chemistry of joints were characterized by scanning electron microscopy, electron probe microanalyses and X-ray diffraction. The results show that some elements of the solder diffuse into silicon nitride to form a diffusion layer. As compared with the joint strength of silicon nitride bonded with  $\text{Y}_2\text{O}_3$ – $\text{Al}_2\text{O}_3$ – $\text{SiO}_2$  solder, the joint strength with  $\text{Y}_2\text{O}_3$ – $\text{La}_2\text{O}_3$ – $\text{Al}_2\text{O}_3$ – $\text{SiO}_2$  solder increased, while the one with  $\text{Y}_2\text{O}_3$ – $\text{CeO}_2$ – $\text{Al}_2\text{O}_3$ – $\text{SiO}_2$  solder decreased. The results indicate that the effect of adhesive composition on joint strength is related to interfacial wetting and joint thickness.

© 2002 Elsevier Science Ltd and Techna S.r.l. All rights reserved.

**Keywords:** D. Silicon nitride; Bonding;  $\text{Y}_2\text{O}_3$ – $\text{Al}_2\text{O}_3$ – $\text{SiO}_2$ ; Joint strength; Interface reaction

## 1. Introduction

Up to now, the most common methods for joining silicon nitride are active metal brazing, diffusion bonding and oxide glass sealing [1]. The joints produced by active metal brazing have high bending strength at room temperature, but are limited to apply below about 1073 K. High joint strength can be obtained by diffusion bonding. However, this method requires an elevated bonding temperature, long joining time and smooth contacting surfaces so it is inadequate for mass production. Satisfactory bonding of silicon nitride with oxide glass solder has been developed [2–9]. However, the elevated temperature strength of joint is limited owing to the lower softening temperature of residual glass in joint. In order to improve the joint strength at elevated temperature, high refractory adhesives must be developed.

It is known that the elevated temperature properties of silicon nitride with additives from the Y–Al system are better than those with additives from the Mg–Al system [10]. To enhance the elevated temperature

properties of silicon nitride ceramic, rare earth oxides such as  $\text{La}_2\text{O}_3$  etc. have been added to the oxide additives of the Y–Al system [11]. Therefore, the bonding of silicon nitride ceramic was carried out with  $\text{Y}_2\text{O}_3$ – $\text{Al}_2\text{O}_3$ – $\text{SiO}_2$ ,  $\text{Y}_2\text{O}_3$ – $\text{La}_2\text{O}_3$ – $\text{Al}_2\text{O}_3$ – $\text{SiO}_2$ ,  $\text{Y}_2\text{O}_3$ – $\text{CeO}_2$ – $\text{Al}_2\text{O}_3$ – $\text{SiO}_2$  mixtures at 1823 K for 15 min, and the effect of adhesive composition on interfacial wetting and joint strength was investigated.

## 2. Experimental procedure

Hot-pressure sintered silicon nitride ceramics, which were provided by Tsinghua University, with bending strength of 700–800 MPa and 19 mm×19 mm×8 mm in size were used. Before bonding, the bonded surfaces of all materials were diamond ground, and cleaned ultrasonically in acetone.  $\text{La}_2\text{O}_3$  and  $\text{CeO}_2$  powders were added to the  $\text{Y}_2\text{O}_3$ – $\text{Al}_2\text{O}_3$ – $\text{SiO}_2$  (YA) mixture, the molar ratio between  $\text{Y}_2\text{O}_3$  and the other rare earth oxide being 1:1. The compositions of YA, YL and YC mixture are listed in Table 1.

The wetting angle of the solder on the ceramic was determined by the sessile drops method. Disks ( $\phi 5$  mm×2 mm) of the three kinds of glass solders were

\* Present address: School of Mechanical Engineering 01, Tohoku University, Sendai, 980-8579, Japan.

E-mail address: zhoufei18@hotmail.com (F. Zhou).

Table 1  
Composition of rare earth oxide glass (percent mass fraction)

Glass solder	La <sub>2</sub> O <sub>3</sub>	Y <sub>2</sub> O <sub>3</sub>	Al <sub>2</sub> O <sub>3</sub>	SiO <sub>2</sub>	CeO <sub>2</sub>
YL	23.63	16.37	20	40	0
YA	0	40	20	40	0
YC	0	22.7	20	40	17.3

placed on the Si<sub>3</sub>N<sub>4</sub> ceramic, and heated in a graphite furnace filled with pure N<sub>2</sub> gas at atmospheric pressure at 1823 K for 15 min. The wetting angle measurement was carried out at room temperature.

The YA, YL and YC mixtures were mixed with acetone to form a homogenous slurry. Then a 0.5 mm thick coating was applied onto a silicon nitride ceramic polished surface by dipping in the slurry. After two coated surfaces were placed together and fixed in a graphite jig coated with boron nitride. The joining was carried out at 1823 K for 15 min in a graphite furnace filled with pure N<sub>2</sub> gas at atmospheric pressure.

The 4 mm×4 mm×38 mm specimens were cut off from the joint perpendicular to the bonded interface for microanalyses and bending tests. The specimen surface for microanalyses was diamond ground and cleaned ultrasonically in acetone. The microstructures and distribution of elements in the joint were identified by

JXA-840A scanning electron microscopes (SEM) and electron probe microanalyses (EPMA), respectively. The fracture surfaces of tested samples were examined by X-ray diffraction (XRD). Four-point bending strength at room temperature was measured with an upper span of 10 mm, a lower span of 30 mm and a cross-head speed of 0.5 mm min<sup>-1</sup>.

### 3. Results and discussion

#### 3.1. Interface microstructure

Fig. 1 shows microstructure and elements distribution in the cross section of Si<sub>3</sub>N<sub>4</sub>/Si<sub>3</sub>N<sub>4</sub> joints bonded with YA mixture at 1823 K for 15 min. The thickness of joint is 40 μm. Some elements of solder (Y<sup>3+</sup>, Al<sup>3+</sup>, O<sup>2-</sup>) diffuse into Si<sub>3</sub>N<sub>4</sub> to form a diffusion layer, while Si<sup>4+</sup> diffuse into the molten glass. This shows that the YA molten glass diffuses into the Si<sub>3</sub>N<sub>4</sub> ceramic along its grain boundary, resulting in Si<sub>3</sub>N<sub>4</sub> dissolution and formation of Y-Sialon glass at the interface. According to XRD analyses of the fracture surface (Fig. 4a), the β-Si<sub>3</sub>N<sub>4</sub> near the interface turned into Si<sub>2</sub>N<sub>2</sub>O gradually at 1823 K, indicating its dissolution into the molten Y-Sialon glass. With the increase of the dissolved Si<sub>3</sub>N<sub>4</sub>

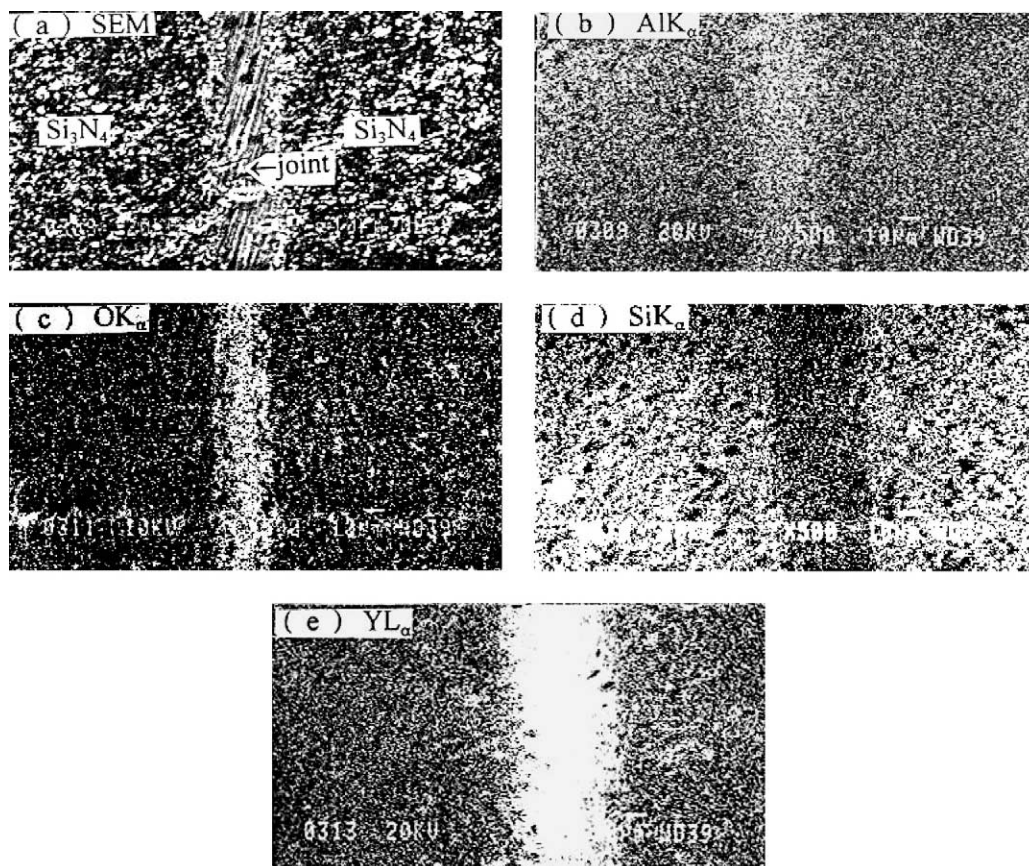


Fig. 1. Microstructure and element distribution images of Al, O, Si, Y for the Si<sub>3</sub>N<sub>4</sub>/Si<sub>3</sub>N<sub>4</sub> joint bonded with YA glass solder at 1823 K for 15 min.

content, the number of non-bridging nitrogen beneficial to crystallization in Y-Sialon glass increases, and thus  $\text{Si}_2\text{N}_2\text{O}$  particles are precipitated from interfacial glass.

Figs. 2 and 3 show microstructure and elements distribution in the cross section of  $\text{Si}_3\text{N}_4/\text{Si}_3\text{N}_4$  joint bonded with YL and YC mixtures at 1823 K for 15 min, respectively. The thickness of joint bonded with YL mixture is 20  $\mu\text{m}$ , while that of YC mixture is 50  $\mu\text{m}$ . Some elements of solder ( $\text{Y}^{3+}$ ,  $\text{Al}^{3+}$ ,  $\text{La}^{3+}$ ,  $\text{Ce}^{4+}$ ,  $\text{O}^{2-}$ ) diffuse into  $\text{Si}_3\text{N}_4$  to form a diffusive layer at interface. The results of XRD analyses on the fracture surface (Fig. 4b and c) show that there are  $\text{LaYO}_3$ ,  $\text{Y}_2\text{Ce}_2\text{O}_7$  phases in joint bonded with YL and YC mixtures, respectively, besides  $\beta\text{-Si}_3\text{N}_4$  and  $\text{Si}_2\text{N}_2\text{O}$ .

In fact, YA, YL and YC liquid glasses diffuse along grain boundary of silicon nitride, penetrate into ceramics, and remain at the triple junctions of grains at 1823 K. This will decrease nitrogen concentration at the grain boundary, which results in the dissolution of  $\beta\text{-Si}_3\text{N}_4$  in the glass. The mean length of Si–N bond in silicon

nitride and that of Si–O bond in silica are 0.174 and 0.162 nm respectively [12]. In silicon oxynitride characterized by  $\text{Si}(\text{O},\text{N})_4$  tetrahedra, the mean length of Si–N bond and Si–O bond are 0.172 and 0.162 nm respectively [12]. It can be seen that the length of corresponding bonds in silicon nitride and silicon oxynitride are equal. This implies that at the interface, the thermodynamically stable  $\text{Si}_2\text{N}_2\text{O}$  crystal can easily precipitate from molten glass. Thus, interfacial reaction could be described as: (a) dissolution of  $\text{Si}_3\text{N}_4$  in molten glass at interface, (b) transfer of Si and N into liquid, (c) precipitation of  $\text{Si}_2\text{N}_2\text{O}$  crystal from liquid.

### 3.2. Effect of solder composition on wetting angle and joint strength

As compared with YA solder, YL solder wetting angle and joint thickness are smaller, but its joint strength is higher. While YC solder wetting angle and joint thickness are larger, but its joint strength is lower

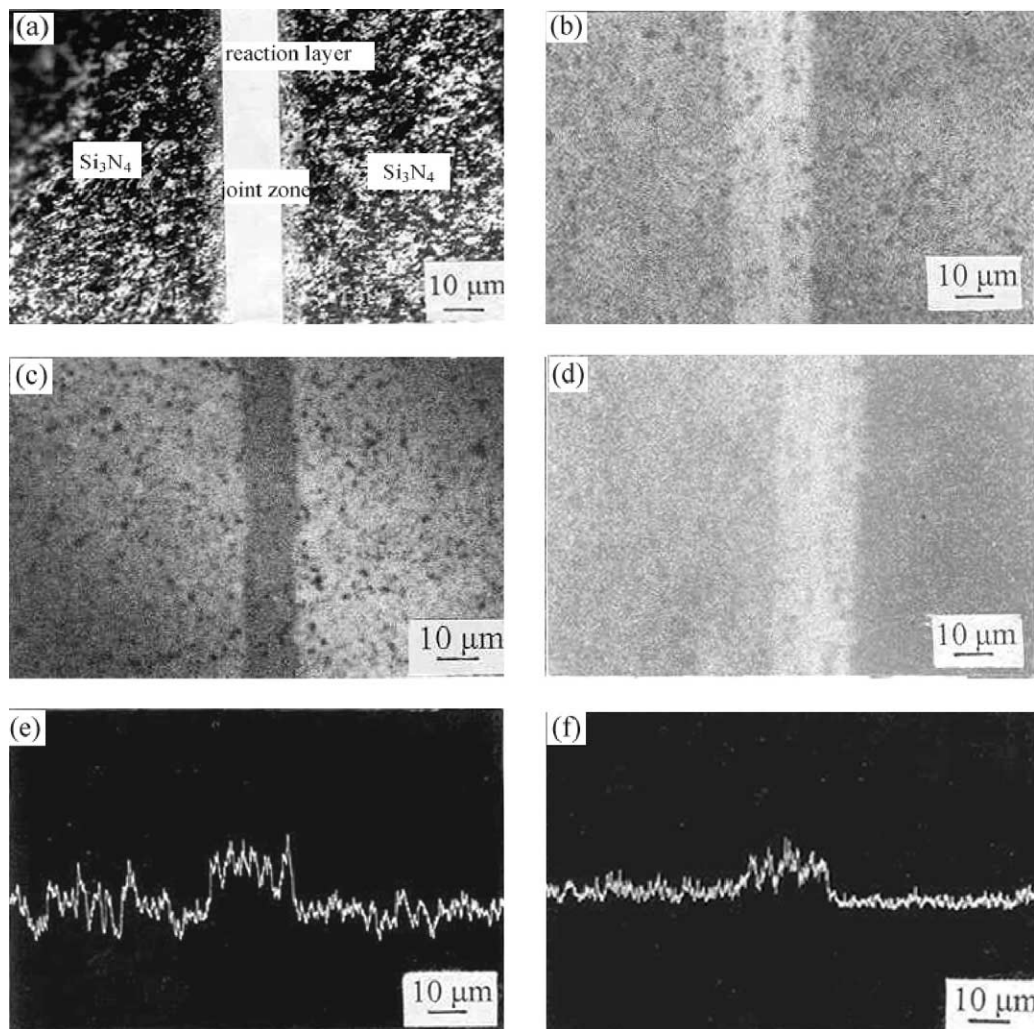


Fig. 2. Microstructure and element distribution images of Al, Ti, Si, La and line distribution images of O, Y for the  $\text{Si}_3\text{N}_4/\text{Si}_3\text{N}_4$  joint bonded with YL glass solder at 1823 K for 15 min: (a) SEM, (b)  $\text{AlK}\alpha$ , (c)  $\text{SiK}\alpha$ , (d)  $\text{LaL}\alpha$ , (e)  $\text{OK}\alpha$ , (f)  $\text{YL}\alpha$ .

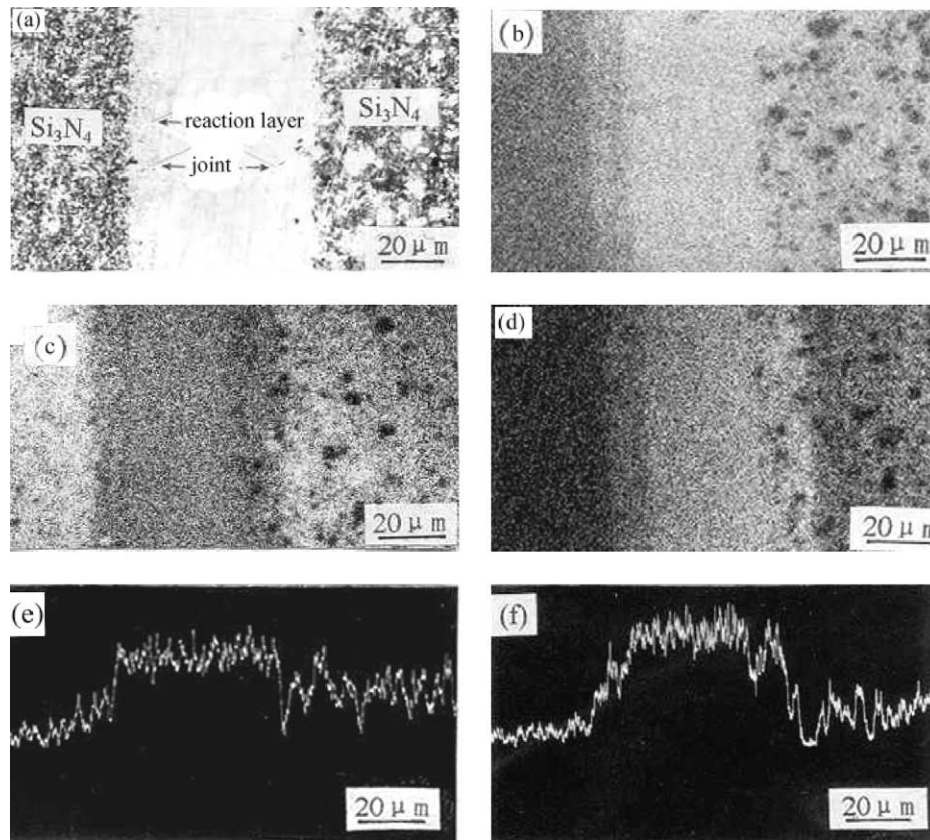


Fig. 3. Microstructure and elements distribution images of Al, Ti, Si, Ce and line distribution images of O, Y for the  $\text{Si}_3\text{N}_4/\text{Si}_3\text{N}_4$  joint bonded with YC glass solder at 1823 K for 15 min: (a) SEM, (b)  $\text{AlK}\alpha$ , (c)  $\text{SiK}\alpha$ , (d)  $\text{CeL}\alpha$ , (e)  $\text{OK}\alpha$ , (f)  $\text{YL}\alpha$ .

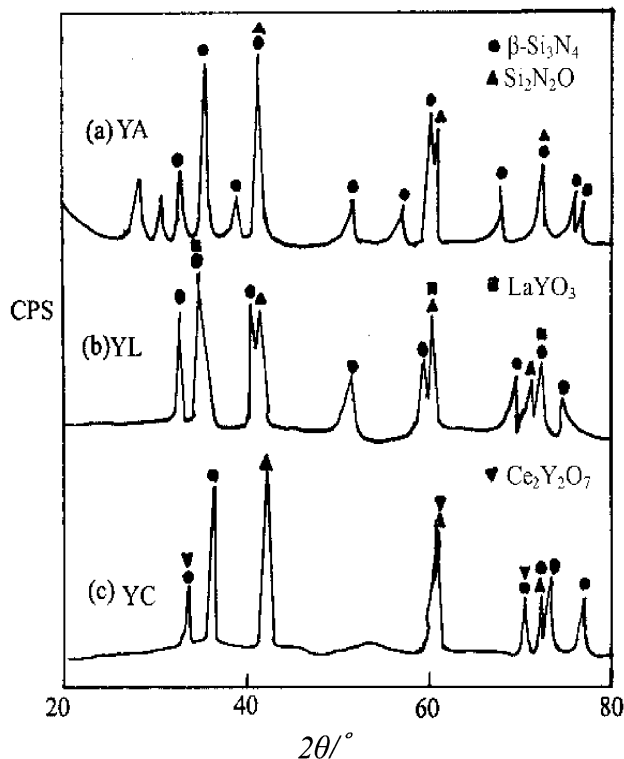


Fig. 4. XRD patterns of fracture surface after bending test.

(as seen in Table 2). The results indicated that  $\text{La}_2\text{O}_3$  addition could improve the wetting behavior of YA glass solder on  $\text{Si}_3\text{N}_4$  ceramic, decreases joint thickness and increases the joint strength. On the contrary  $\text{CeO}_2$  addition would deteriorate the wetting ability of YA glass solder on  $\text{Si}_3\text{N}_4$  ceramic, and joint thickness increases will decrease joint strength.

It is evident from Table 2 that YL liquid solder diffusion and infiltration into  $\text{Si}_3\text{N}_4$  ceramic is easier than for YA liquid solder, while YC liquid solder diffuses and infiltrates into  $\text{Si}_3\text{N}_4$  ceramic more difficultly than YA liquid solder does. In fact, the migration of solid/liquid interface is governed by the grain-boundary capillary effect of ceramic when the bonding of ceramic is carried out with glass solder at atmospheric pressure [7], and the joint thickness is expressed as [13]:

$$w_t = w_0 - \sqrt{2}f_v \left( \frac{\gamma \cos \theta}{\eta} rt \right)^{\frac{1}{2}} \quad (1)$$

where  $w_0$  is initial joint thickness at bonding temperature  $T$ ,  $w_t$  is joint thickness as holding time is  $t$  at bonding temperature  $T$ ,  $f_v$  is capillary area fraction on the bonding surface of ceramic,  $r$  is radius of the grain-boundary capillary,  $\gamma$  is interface energy between liquid solder and ceramic,  $\eta$  is viscosity of liquid solder,  $\theta$  is

Table 2  
Effect of solder composition on wetting angle, joint strength and thickness

Glass solder	Wetting angle (°)	Joint strength (MPa)	Joint thickness (μm)
YA	18±2	315±10	40±2
YL	5±0.5	350±15	20±1.2
YC	38±3	280±10	50±2.5

wetting angle of liquid solder on ceramic at bonding temperature  $T$  for holding time  $t$ . In the case of the same bonding technique and ceramic, the joint thickness is mainly related to the viscosity and wetting angle of liquid solders and interface energy.

Menon and Chen [14] indicated that the wetting behavior of oxide glass on nitride ceramic is affected by the basicity of oxide glass. It is easy for strong basicity oxide glass to wet silicon nitride ceramic. For rare earth aluminosilicate glass, its basicity is related to the basicity of rare earth metal oxide [14]. According to Wen's theory [15], the basicity of rare earth metal oxide is judged by the formation energy parameter of rare earth metal ion. The higher the formation energy parameter of metal ion, the stronger the basicity of metal ion. As seen in Table 3, it is clear that the basicity of  $\text{La}_2\text{O}_3$  and  $\text{Ce}_2\text{O}_3$  is stronger than that of  $\text{Y}_2\text{O}_3$  and  $\text{CeO}_2$ , respectively. If another rare earth metal oxide is added to YA glass solder, the mean parameter of formation energy for rare earth metal ions in glass is [13]:

$$\overline{w_f} = \frac{\sum_{i=0}^n x_i n_i w_{fi}}{\sum_{i=0}^n x_i n_i} \quad (2)$$

where  $x_i$  is the molar fraction of  $i$  rare earth metal oxide in all rare earth metal oxide of glass,  $n_i$  is the number of rare earth metal ion in  $i$  rare earth metal oxide,  $w_{fi}$  is the formation energy parameter of rare earth metal ion in  $i$  rare earth metal oxide. When  $\text{CeO}_2$  is added to YA glass solder, the mean formation energy parameter for rare earth metal ions in glass is 15. Then YC glass solder wetting ability is not improved, which is in agreement with the results of the wetting test (as seen in Table 2). Moreover, In  $\text{Y}_2\text{O}_3\text{--RE}_2\text{O}_3$  ( $\text{REO}_2$ ) system,  $\text{Y}_2\text{O}_3$  easily reacts with  $\text{RE}_2\text{O}_3$  ( $\text{REO}_2$ ) to form compounds if the ion radius difference between  $\text{Y}^{3+}$  and  $\text{RE}^{3+(4+)}$  is small [16]. The ion radius of  $\text{Ce}^{4+}$ ,  $\text{Y}^{3+}$  and  $\text{Ce}^{3+}$  being 0.092, 0.090 and 0.101 nm, respectively,  $\text{CeO}_2$  more easily reacts with  $\text{Y}_2\text{O}_3$  to form  $\text{Ce}_2\text{Y}_2\text{O}_7$  than  $\text{Ce}_2\text{O}_3$

although  $\text{CeO}_2$  may be transformed into  $\text{Ce}_2\text{O}_3$  at elevated temperature [17]. Therefore, the poor wetting ability of YC glass solder and the high viscosity of liquid solder caused by the phase formation would make the joint thickness increase, and then a tensile stress was formed easily at midplane of joint [19], which led to a joint strength decrease.

As  $\text{La}_2\text{O}_3$  is added to YA glass solder, the mean formation energy parameter for rare earth metal ions in glass is 21, which shows that the basicity of YL glass solder is stronger than that of YA glass solder. Then the YL glass solder wetting ability on silicon nitride ceramic is better than for YA glass solder, which is consistent with the results of the wetting test. Moreover, after  $\text{La}_2\text{O}_3$  is added to YA glass solder, it will expand the glass formation region, and decrease the viscosity of the molten glass [18]. As a result, the better wetting ability of YL glass solder on silicon nitride ceramic and the lower viscosity of glass solder will make the joint thickness decrease, and then the residual thermal stress at joint is relaxed [19], which is beneficial to joint strength.

#### 4. Conclusions

1. Interfacial reaction could be described as: (a) dissolution of  $\text{Si}_3\text{N}_4$  in molten glass at interface, (b) transfer of Si and N into liquid, (c) precipitation of  $\text{Si}_2\text{N}_2\text{O}$  crystal from liquid.
2.  $\text{La}_2\text{O}_3$  addition could improve the YA glass solder wetting behavior on  $\text{Si}_3\text{N}_4$  ceramic, and then enhance the joint strength, while  $\text{CeO}_2$  addition would deteriorate the YA glass solder wetting ability on  $\text{Si}_3\text{N}_4$  ceramic, and then lead to the decrease of the joint strength.

#### References

- [1] F. Zhou, Progress in joining of silicon nitride ceramic, Bull. Chin. Ceram. Soc. 41 (2) (1997) 41–47.
- [2] M.L. Mecarteny, R. Sinclair, R.F. Loehman, Silicon nitride joining, J. Am. Ceram. Soc. 68 (9) (1985) 472–479.
- [3] M. Johnson, D.J. Rowcliffel, Mechanical properties of joined silicon nitride, J. Am. Ceram. Soc. 68 (9) (1985) 486–491.

Table 3  
Formation energy parameters for rare earth metal ions  $w_f$  [16]

Metal ions	$\text{La}^{3+}$	$\text{Ce}^{3+}$	$\text{Y}^{3+}$	$\text{Ce}^{4+}$
$w_f$	28	27	15	15

- [4] F. Zhou, Z. Li, Q. Luo, Bonding of silicon nitride ceramic composite with  $\text{RE}_2\text{O}_3\text{--Al}_2\text{O}_3\text{--SiO}_2$  glass solders, *J. Rare Earth* 17 (3) (1999) 194–199.
- [5] F. Zhou, Effect of 4th element on bonding of silicon nitride ceramic with  $\text{Y}_2\text{O}_3\text{--Al}_2\text{O}_3\text{--SiO}_2$  glass solder, *J. Rare Earth* 19 (2) (2001) 90–96.
- [6] S.J. Glass, F.M. Mahoney, B. Quillan, J.P. Pollinger, R.E. Loehman, Refractory oxynitride joints in silicon nitride, *Acta Mater.* 46 (7) (1998) 2393–2399.
- [7] S. Baik, R. Raj, Liquid-phase bonding of silicon nitride ceramics, *J. Am. Ceram. Soc.* 70 (1) (1987) c105–108.
- [8] Y. Owada, K. Kobayashi, Joining of silicon nitride ceramics, *J. Ceram. Soc. Jpn.* 92 (12) (1984) 693–699.
- [9] P.A. Walls, M. Ueki, Joining of sialon ceramic using composite  $\beta$ -sialon-glass adhesives, *J. Am. Ceram. Soc.* 75 (9) (1992) 2491–2498.
- [10] K.H. Jack, Sialon and related nitrogen ceramics, *J. Mater. Sci.* 11 (1976) 1135–1142.
- [11] Y. Chen, L.P. Huang, X.W. Sun, Effect of sintering additives on high temperature properties of silicon nitride ceramics, *J. Ceram. Soc. Chin.* 25 (2) (1997) 183–186.
- [12] H.P. Huang, P. Bill, Effect of oxide additives on formation of  $\text{Si}_3\text{N}_4\text{O}$  powder, *J. Inorg. Mater.* 6 (4) (1991) 421–428.
- [13] F. Zhou, Effect of heat treatment on joint strength of silicon nitride ceramic composite, *Trans. Metal Heattreatment* 20 (suppl) (1999) 511–513.
- [14] M. Menon, I.W. Chen, Reaction densification of  $\alpha'$ -sialon: I, wetting behavior and acid-base reaction, *J. Am. Ceram. Soc.* 78 (3) (1995) 545–552.
- [15] Y.K. Wen, J. Shao, S.S. Wang, A simplified formula to calculate heat of formation of oxyacid salt and mineral, *Acta Metall. Sinica* 15 (3) (1979) 98–109.
- [16] N. Hirotsaki, A. Okada, K. Matoba, Sintering of  $\text{Si}_3\text{N}_4$  with the addition of rare-earth oxides, *J. Am. Ceram. Soc.* 71 (3) (1988) c144–147.
- [17] S.L. Lin, C.S. Hwang, Structures of  $\text{CeO}_2\text{--Al}_2\text{O}_3\text{--SiO}_2$  glasses, *J. Non-Cryst. Solids* 20 (2) (1996) 61–67.
- [18] J.E. Shelby, J.T. Kohli, Rare earth aluminosilicate glass, *J. Am. Ceram. Soc.* 73 (1) (1990) 39–43.
- [19] F. Zhou, Z. Li, Q. Luo, Influence of bonding conditions on joint strength of  $\text{Si}_3\text{N}_4/\text{Si}_3\text{N}_4$  bonding, in: *Asian Pacific Conference for Fracture and Strength*, Xi'an, 1999, pp. 490–495.